Supplementary Materials for: Structural and topological changes across the liquid-liquid transition in water

Riccardo Foffi, John Russo, Francesco Sciortino

Equilibration and sampling

At low temperatures it is of crucial importance to ensure that MD simulations are long enough for the system to equilibrate, and that equilibrated configurations are sampled with a large enough timestep for them to decorrelate. In order to minimize possible artifacts due to equilibration and correlation we have been quite conservative in analyzing our simulation data. Simulation and equilibration times adopted for each simulation are reported in Tab. S1. Since molecular mobility is affected by pressure, low-pressure simulations(1 and 1000 bar) were run for longer times than high-pressure simulations(2500 and 4000 bar); the two systems close to phase coexistence(1800 bar) were run for a longer time in order to ensure that neither of them would transit to the other phase, so that while one of them must be metastable with respect to the other, the lifetime of this metastable state is long enough to be considered effectively stable. In the production phase, configurations were then sampled every 80 ns.

The two simulations at 1900 bar(shown in Fig. 1 for reference) have not been used for the structural analysis since their data at equilibrium is redundant with the high-density 1800 bar simulation; thus they are not reported here.

Table S1: Total simulation time and equilibration times adopted for each explored state point. Samples in the production phase were collected at intervals of 80 ns.

pressure / bar	simulation time / µs	equilibration time / µs
1	28	25
1000	13	10
1800 (LDL)	26	23
1800 (HDL)	23	20
2500	10	7
4000	4	1

Properties of real and inherent structures

All the structural analysis reported in the main text was performed on the inherent structures(IS) of the system. It is worthwhile to prove that the structural features we observe are genuine properties of the model and do not arise only as a result of this energy minimization procedure. This is accomplished by reproducing some of the structural results using configurations extracted from the real dynamics (RS).

Fig. S1 shows the joint orientation-distance distribution of water molecule pairs in the two coexisting systems at 188 K and 1800 bar, evaluated in the RS; these plots have to be compared to Fig. 2 in the main text, where the same distributions are evaluated in the IS. Even though we are at a very low temperature, the effects of thermal distortion are clearly observable; the well-defined islands of Fig. 2 now morph into broad and overlapping regions.

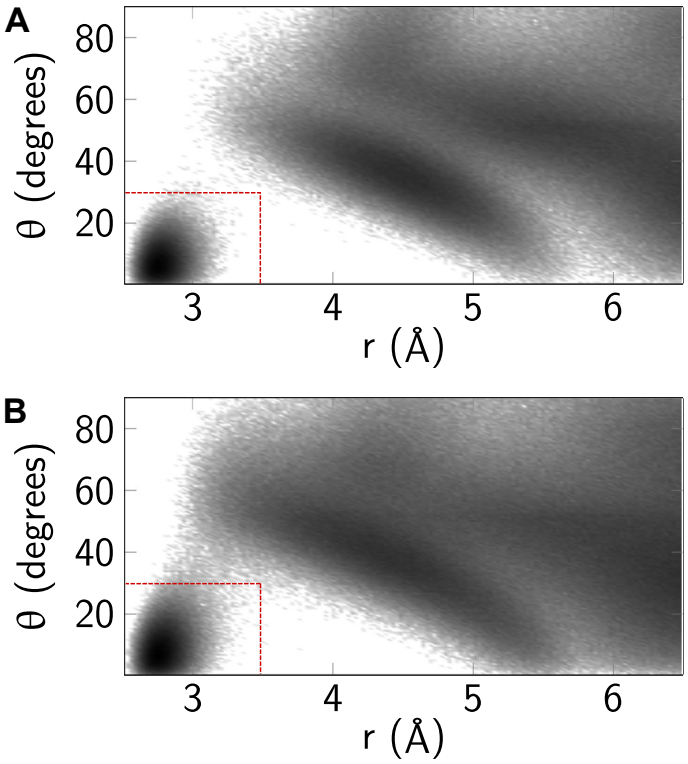

Figure S1: Joint orientation-distance distribution of water molecule pairs evaluated on the real structures in the (**A**) LDL and (**B**) HDL phases at $T = 188\,\mathrm{K}$ and $P = 1800\,\mathrm{bar}$. The probability density $P(r, \theta)$ is shown in log scale. Dashed red lines show the boundaries defined by our notion of H-bond.

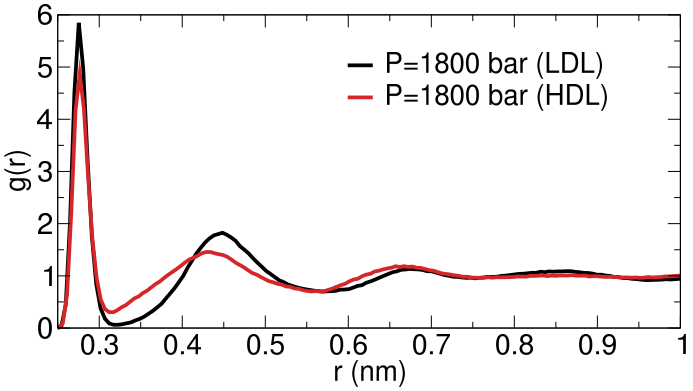

Figure S2: Oxygen-oxygen radial distribution functions in the coexisting LDL and HDL states at 188 K and 1800 bar, evaluated in the real structures.

In the LDL(panel A) we can still clearly discern the region associated to H-bonds to be well separated from the outer shells, while in the HDL(panel B) the definition of HB seems to be somewhat ill-defined, in the sense that our tresholds cut through a populated region. However it should be kept in mind that the $P(r, \theta)$ being shown in log scale accentuates weakly-populated regions, so that the overlap generally looks worse than it actually is.

Quantitatively, we estimate the error associated to this definition of HB as follows: we consider "ambiguous" bonds those that are within the HB distance threshold $r < 3.5\,\text{Å}$ and within 20% above of the angular threshold $30° < \theta < 36°$, and the average error is then defined as the ratio between the number of ambiguous bonds and the number of "sure" bonds(i.e. those within the cutoffs). In the LDL we find an average error of $\sim 0.2\%$, against $\sim 0.8\%$ in the HDL. That is, in

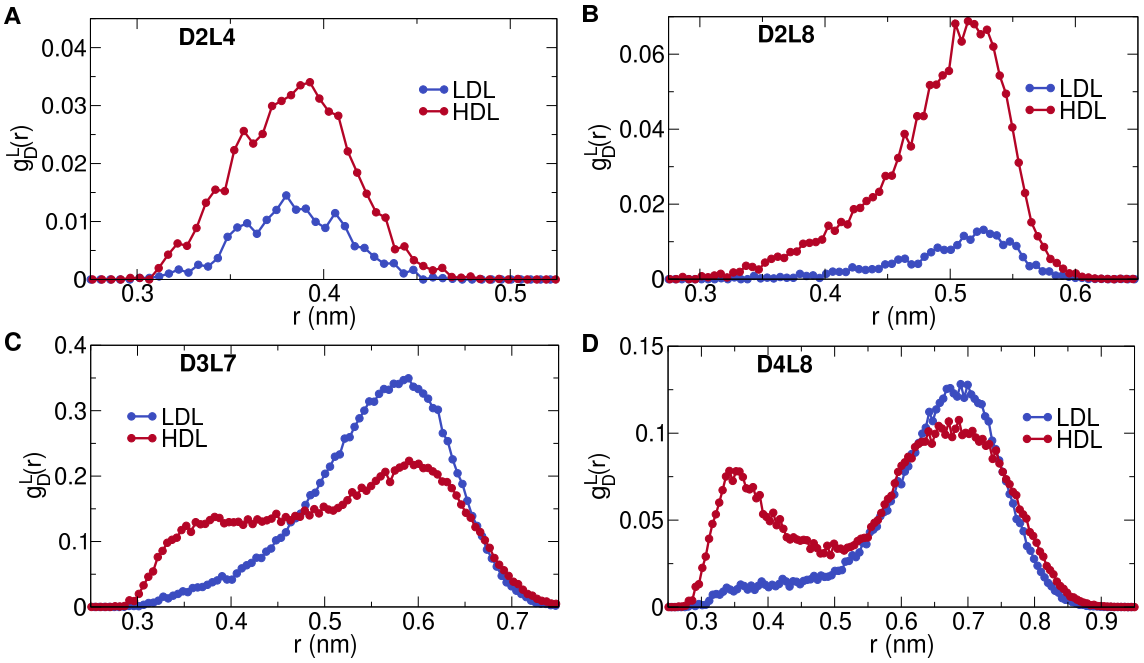

Figure S3: Contributions to the $g(r)$ of the real structures in the two liquid phases at coexistence (188 K and 1800 bar) arising from (**A**) D2L4, (**B**) D2L8, (**C**) D3L7 and (**D**) D4L8 rings

.

both systems we miss less than 1 HB every 100, which means that at the explored thermodynamic conditions, the identification of H-bonds is robust even in the RS.

To show that the structure of the liquid is not fundamentally altered by the instantaneous quenching, we also reproduce the oxygen-oxygen radial distribution functions $g(r)$ of the two coexisting states in the RS, shown in Fig. S2, to be compared with Fig. 5A from main text. Clearly, due to the thermal distortion the $g(r)$ evaluated in the RS shows broader peaks with respect to the IS, but the overall structural features are unchanged: the growth in the population of interstitial molecules in the HDL can still be clearly discerned. The main differences between IS and RS, as could be expected from Fig. S1, are observed in the first bond-coordination shell, corresponding to the optimization of H-bonds that gives rise to an extremely tight and tall first peak. The net effect of the energy minimization decays with increasing distance and eventually dies out in the long range limit.

If we are able to meaningfully identify H-bonds and the overall liquid structure is unaffected by the energy minimization, then we can also apply our topological classification, based on chemical distance and ring length, to the RS. The results of our topology-based partitioning of the $g(r)$ on the RS are shown in Fig. S3, corresponding to Fig. 11 in main text. It is clear that the partitioning works despite thermal distortion, and the RS results are consistent with those in the IS.

Extended pressure effect in $g(r)$ and $S(q)$

We show here the oxygen-oxygen $g(r)$ and $S(q)$ for the entire explored pressure range, from 1 bar to 4000 bar, both in the IS and the RS. The increase in pressure(and therefore density) is accompanied by a progressive shift of the first diffraction peak to larger q values and a weakening of the second diffraction peak. The characterising features of the transition in real space can be identified in the increase in the number of interstitial molecules ($r \approx 0.35$ nm) along with the decay of the tetrahedral ordering that defines the second peak. It is clearly observed that at all thermodynamic conditions, the IS is only characterized by minor corrections with respect to the RS, related to a "refinement" of the H-bonds. The most relevant effect, as can be expected, is the short-range structure associated to ordering in the first neighbor shell: consistently with Fig. S1,

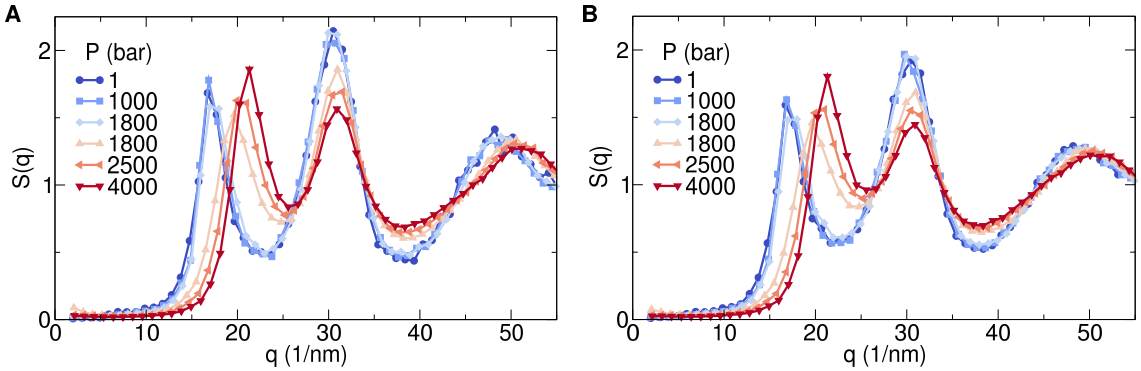

Figure S4: Oxygen-oxygen structure factor of water evaluated along the 188 K isotherm in (**A**) IS and (**B**) RS.

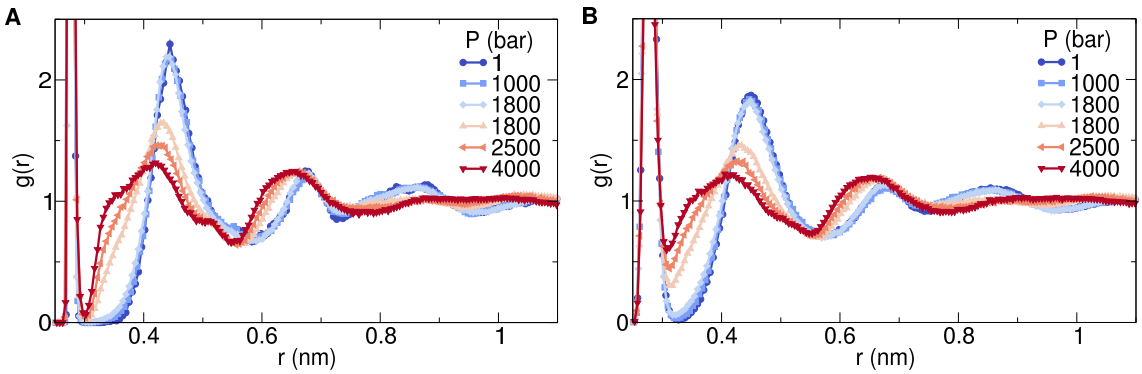

Figure S5: Oxygen-oxygen radial distribution function of water evaluated along the 188 K isotherm in (**A**) IS and (**B**) RS.

the RS show a broader first peak in the $g(r)$. This difference however does not significantly affect the structural analysis; the fundamental structural features of the system are unaltered by energy minimization.